

NANO EXPRESS

Open Access



A Convenient Ultraviolet Irradiation Technique for Synthesis of Antibacterial Ag-Pal Nanocomposite

Shuai Han^{1,3}, He Zhang², Lianwei Kang¹, Xiaoliang Li¹, Chong Zhang¹, Yongjie Dong¹ and Shenjun Qin^{1,3*}

Abstract

In the present work, palygorskite (Pal) was initially subjected to an ion-exchange reaction with silver ions (Pal-Ag⁺). Subsequently, Ag-Pal nanocomposites were assembled by a convenient ultraviolet irradiation technique, using carbon dots (CDs) derived from wool fiber as the reducing agent. The obtained nanocomposites were characterized by powder X-ray diffraction (XRD), ultraviolet-visible (UV-vis) spectroscopy, transmission electron microscopy (TEM), and Fourier transform infrared spectroscopy. The XRD patterns and UV-vis absorption spectra confirmed the formation of the Ag nanoparticles (NPs). Meanwhile, the TEM images showed that the Ag NPs, which exhibited sizes in the range of 3–7 nm, were located on the surface of the Pal nanofiber structures. Furthermore, the antibacterial activity of the nanocomposites was evaluated against Gram-positive (*Staphylococcus aureus*) and Gram-negative (*Escherichia coli*) bacteria by applying the disc diffusion method and minimum inhibitory concentration test. Owing to their good antibacterial properties, the Ag-Pal nanocomposites are considered to be a promising bactericide with great potential applications.

Keywords: Palygorskite, Carbon dots, Ag NPs, Nanocomposite, Antibacterial activities

Background

Among the various materials used for antimicrobial activities, nanostructured materials are considered to be more effective because of their high surface-area-to-volume ratio [1–3]. Additionally, the use of inorganic nanoparticles (NPs) as antimicrobial agents has several benefits, such as improved stability and safety, compared with the use of organic antimicrobial agents [4, 5]. Typical inorganic NPs consist of Ag, Cu, ZnO, TiO₂, SnO₂, and CuO [6].

Ag NPs have been reported to be an effective antimicrobial agent; they have been widely used in a broad spectrum of applications including water purification, wound care, and food production [7, 8]. However, free Ag NPs without a supporting matrix might be inadequate for applications where prolonged Ag release is needed (e.g., in medical devices) [9]. On the other hand, the small

size of the NPs favors their aggregation, which might cause disadvantageous changes in their chemical, physical, and antibacterial properties [10]. To overcome these issues, hybrid processes combining Ag NPs with other environmentally friendly, inert, and cheap materials are adopted to fully exploit their properties in various applications [11].

Among the possible matrices, clay minerals are particularly attractive because of their cost effectiveness and widespread availability [12, 13]. Palygorskite (Pal), a member of the clay group, is a hydrated magnesium aluminum silicate with reactive hydroxy groups on the surface [14]. Pal consists of a three-dimensional network of densely packed rods; the single rod crystal is the smallest structure unit with a length in the range of 200–500 nm and a diameter of 10–25 nm [15]. Owing to the special nanostructure, inherent stability, and large specific surface area, considerable effort has been devoted to discover new approaches of using Pal in its native and modified forms [16–18].

Composites of metal NPs supported on clay can be fabricated by using various techniques, such as ion-exchange

* Correspondence: qsjhbhd@163.com

¹College of Science, Hebei University of Engineering, Handan 056038, Hebei, People's Republic of China

³Hebei Collaborative Innovation Center of Coal Exploitation, Hebei University of Engineering, Handan 056038, People's Republic of China

Full list of author information is available at the end of the article

processes, solvothermal synthesis, chemical reduction methods, and sol-gel processes [19]. However, the development of a simple and green synthetic method with environmentally friendly reagents still represents a great challenge [20]. As an emerging class of carbon nanomaterials, carbon dots (CDs) have drawn much attention due to their outstanding photostability, low environmental risk, high biocompatibility, and interesting electron transfer behavior [21–23]. In recent years, significant research efforts have been dedicated to produce noble metal NPs using CDs as the reducing agent [24, 25], providing new opportunities for the synthesis and applications of metal nanomaterials [26].

In the present work, wool fiber, a cheap and abundant bioresource, was used to fabricate wool fiber-derived CDs (WCDs) by a hydrothermal method. Then, using the obtained WCDs as a reducing agent, Ag-Pal nanocomposites were fabricated by ultraviolet (UV) radiation method, which is a simple and green process (90 min exposure to a UV lamp). The composites were then characterized by transmission electron microscopy (TEM), X-ray diffraction (XRD), and Fourier transform infrared (FTIR) spectroscopy. Finally, the antibacterial activity of the nanocomposites was evaluated using the minimum inhibitory concentration (MIC) test and Kirby-Bauer disk diffusion method. Owing to the excellent antibacterial properties against both Gram-positive (*Staphylococcus aureus*) and Gram-negative (*Escherichia coli*) bacteria, the Ag-Pal nanocomposite is considered a promising bactericide with great potential applications.

Methods

Materials

Pal (Jiangsu Autobang Co., Ltd., China) was treated with HCl and H₂O₂ to remove the impurities and activate the hydroxyl groups on the surface [27]. AgNO₃ was obtained from Aladin Ltd. (Shanghai, China). *E. coli* (ATCC 25,922) and *S. aureus* (ATCC 25,923) were purchased from China General Microbiological Culture Collection Center (Beijing, China). Deionized (DI) water was used for the experiments.

Methods

TEM was performed on a JEOL-2010 TEM (Japan) at 200 kV. FTIR spectra were collected within the 4000–400 cm⁻¹ wavenumber range using a Nicolet 360 FTIR spectrometer with the KBr pellet technique. Nitrogen (N₂) adsorption-desorption isotherms were measured by an ASAP 2010 analyzer with N₂. Powder XRD (PXRD) patterns were obtained with a Rigaku-Dmax 2400 diffractometer using Cu-K α radiation in the 2θ range of 5°–70°. UV-visible (UV-vis) spectra were recorded using a Perkin-Elmer Lambda 20 UV-vis spectrometer. Excitation and emission spectra were collected using a Hitachi

F-4500 Fluorescence spectrophotometer. Quantitative determinations of Ag were obtained by inductively coupled plasma optical emission spectrometry (ICP-OES; IRIS Advantage ER/S spectrophotometer). The UV-vis absorption spectra were recorded on a Perkin-Elmer Lambda 950 spectrophotometer.

Synthesis of the WCDs

WCDs were prepared by the hydrothermal treatment of wool fibers. In a typical synthesis, 0.4 g of wool fibers was transferred into a 100 mL Teflon-lined stainless steel autoclave and heated at 180 °C for a period of 12 h. When the reaction was completed, the autoclave was cooled down naturally. The resulting light yellow solution was centrifuged at 16,000 rpm for 30 min to remove the large dots, yielding a light brown aqueous solution of WCDs (yield ~36.5 %).

Preparation of the Ag Ion-Exchanged Pal (Pal-Ag⁺)

A 25 mg of AgNO₃ was dissolved in 25 mL of DI water. Next, 200 mg of Pal was subjected to the ion-exchange process in a AgNO₃ solution at 25 °C for 5 h with continuous stirring. At the end of the reaction, Pal-Ag⁺ was collected by centrifugation at 8000 rpm for 30 min. The product was then dried at 80 °C overnight. It could be shown from the EDX that the concentration of elemental silver varied from 3.0 to 8.7 % for the product (Additional file 1: Figure S1), which indicated the formation of Pal-Ag⁺.

Fabrication of the Ag-Pal Nanocomposite

Part of Pal-Ag⁺ (40 mg) was dispersed in ethanol by ultrasonic process; 4 mg of WCDs was added. Then, the mixture was placed in a UV quartz cuvette (1 × 1 × 5 cm) located 3 cm away from a 6 W UV lamp (Vilber Lourmat). After the photoreaction (254 nm, 50 min), the color of the solution changed from light yellow to dark brown, implying the formation of the Ag-Pal nanocomposite (Additional file 2: Figure S2).

Antimicrobial Tests

E. coli and *S. aureus* were cultivated in a beef extract peptone medium at 37 °C for 12 h with a shaking incubator. The disk diffusion test was performed according to a reported procedure [28], while equal amounts of Pal-Ag⁺ and Ag-Pal nanocomposites (200 ± 10 μg) were loaded into the filter papers. The bacterial suspension (100 μL of 10⁴–10⁵ CFU mL⁻¹) was applied uniformly on the surface of the nutrient agar plates. Then, the disks were placed on the plates and incubated at 35 °C for 24 h. After the incubation period, the zones of inhibition were measured and digital images of the plates were captured. For the minimum inhibitory concentration (MIC) test, the survival of the organisms was observed by visual inspection as recorded [29].

Leaching Test

To evaluate the stability of the Ag-Pal nanocomposite, leaching tests were performed. Typically, 0.2 g of nanocomposite was dispersed in 20 mL of DI water and vigorously shaken in a shaking thermostatic bath (30 °C, 200 rpm) for various time periods. After shaking, the suspensions were centrifuged at 8000 rpm for 20 min. The supernatant was analyzed using ICP-OES to establish the quantity of Ag leached into the water.

Results and Discussion

Characterization of WCDs

The low-resolution TEM image (Fig. 1a) shows that the as-synthesized WCDs are uniform in size (average diameter of 1–5 nm) and exhibit a nearly spherical shape. The high-resolution TEM image reveals the lattice fringes of WCDs to be 0.206 nm (Fig. 1a), which corresponds to the [102] facet of graphitic (sp^2) carbon [30]. The FTIR spectra of the WCDs are shown in Fig. 1b. The peak between 3200 and 3700 cm^{-1} is assigned to the stretching of the O–H and N–H bonds, while the peaks at 2923 and 2850 cm^{-1} are ascribed to the stretching of the C–H

bond. The peak at 2350 cm^{-1} is assigned to the stretching of O–H and C–N bonds. The peaks at 1635, 1570, and 1420 cm^{-1} can be identified as the stretching of the C=O group, the bending of the N–H bond, and the stretching of the C=C group, respectively [31–33]. Owing to the aromatic π system and the n– p^* transition of the carbonyl, the UV-vis spectrum of the obtained WCDs (Fig. 1c) exhibits a broad absorption band centered at 274 nm [34]. Similar to the previous reports, excitation-dependent photoluminescence (PL) was also observed for the WCDs (Fig. 1d) [35].

Characterization of the Ag-Pal Nanocomposite

The PXRD patterns of Pal and the Ag-Pal nanocomposite are shown in Fig. 2. The Pal characteristic peaks appear at 2θ values of 8.5, 19.7, 26.6, 34.5, and 42.3°, which are consistent with those in other reports [36]. For the Ag-Pal nanocomposite, the peaks are evident and almost identical (Fig. 2). This phenomenon indicates that the structure of Pal was maintained after the modification. However, a new peak was observed corresponding to the formation of Ag NPs in the

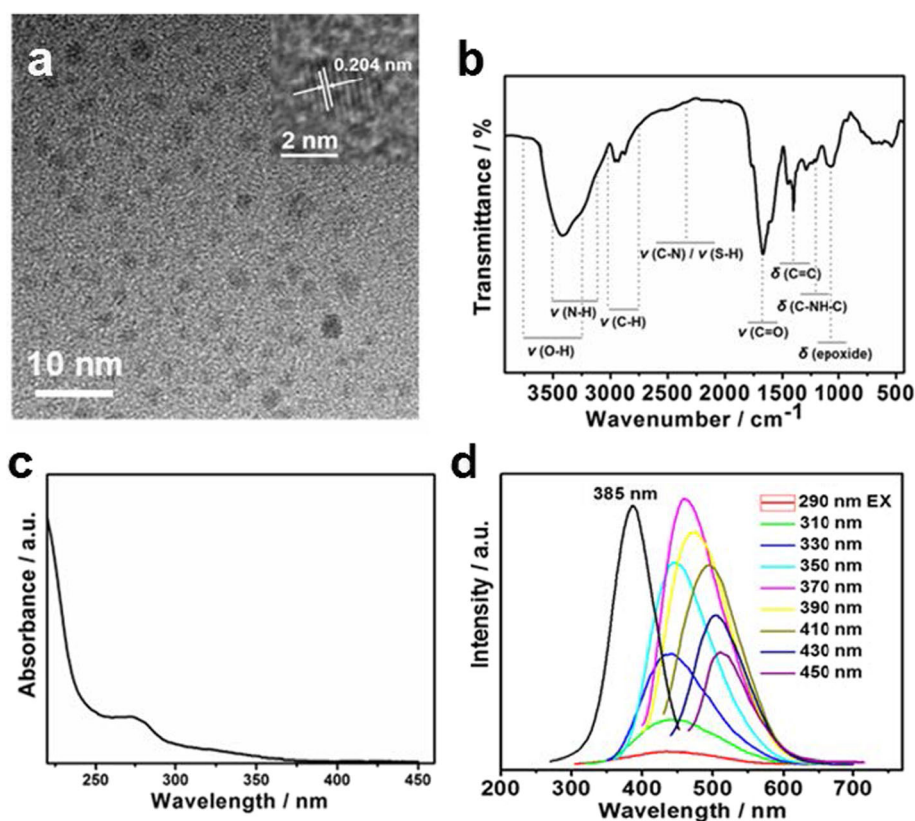
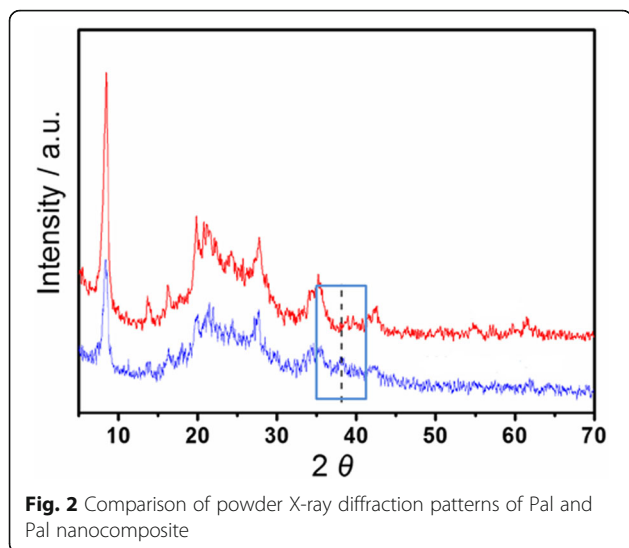
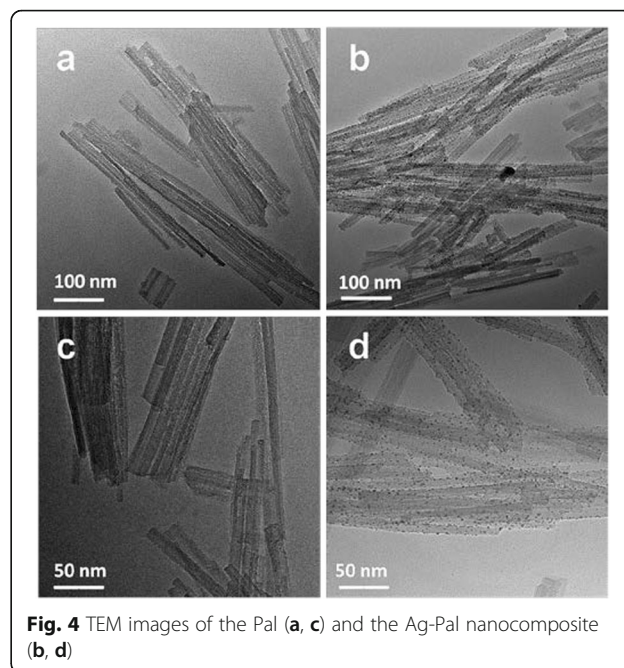
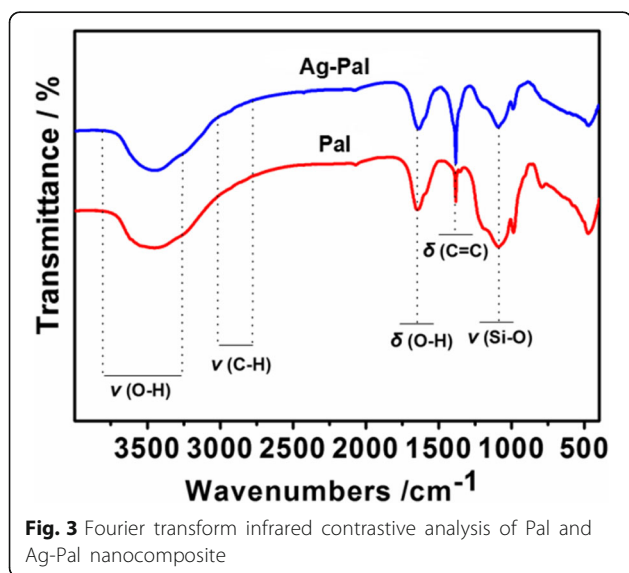


Fig. 1 **a** Transmission electron microscopy (TEM) image (*inset*: high-resolution TEM image), **b** Fourier transform infrared spectrum, **c** ultraviolet-visible absorption spectra, and **d** excitation-dependent photoluminescence spectra of WCDs; the excitation was monitored at the maximum emission peak of 455 nm (*black line*)



nanocomposite. The peak appeared at $2\theta = 38^\circ$ and can be attributed to the (111) crystallographic planes of the face-centered cubic Ag crystals [37]. The UV-vis absorption spectrum of the Ag-Pal nanocomposite is shown in Additional file 3: Figure S3. Notably, an absorption band with a maximum at 415 nm, corresponding to the spectral behavior of Ag crystals, can be observed, supplying new evidence of the formation of Ag NPs [38].

The FTIR spectra of Pal and Ag-Pal nanocomposite are shown in Fig. 3. The most intense band in the FTIR spectra of Pal appeared at 1043 cm^{-1} and was attributed to the Si–O in-plane stretching vibration. The broad bands at 1645 and 3456 cm^{-1} were attributed to the bending and stretching vibrations, respectively, of the hydroxyl groups of the water molecules present in the clay [39].



However, all the bands in the Ag-Pal nanocomposite spectrum decreased in intensity, compared to those of the Pal matrix, indicating that the Ag NPs interacted with the surface of the Pal support. On the other hand, a clear increase of the intensity of the band at 1420 cm^{-1} was observed, which might be attributed to the stretching of the WCD C=C bond in the nanocomposites.

The TEM micrographs of Pal and Ag-Pal are shown in Fig. 4. After the modification, many small spherical NPs appeared on the surface of the Pal nanofiber structures (Fig. 4b, d); according to the XRD and FTIR results, these particles were identified as Ag NPs. The mean diameter of the Ag NPs was determined to be $\sim 3\text{--}7\text{ nm}$. Energy dispersive X-ray spectroscopy (EDX) was further used to analyze the elemental constitution of the Pal and Ag-Pal (Fig. 5). It is shown from Fig. 5a that silicon, magnesium, and aluminum were the principal elements present for the Pal. After the ultraviolet radiation reaction, new peak at 3.9 keV was observed corresponding to the silver element in the nanocomposite (Fig. 5b). It could be also obtained from the EDX that the concentration of elemental silver varied from 3.2 to 8.8 % for the Ag-Pal nanocomposite.

Antibacterial Properties of the Ag-Pal Nanocomposite

The antibacterial properties of the Ag-Pal nanocomposite against Gram-negative (*E. coli*) and Gram-positive (*S. aureus*) bacteria were examined using the disk diffusion method and MIC test; Pal-Ag⁺ was used as the contrast material for the comparison of the activity. As shown in Fig. 6a, b, the disks with Ag-Pal were surrounded

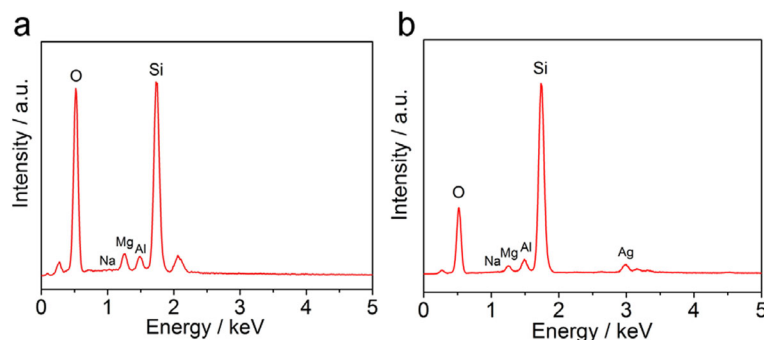


Fig. 5 EDX spectrum of Pal (a) and Ag-Pal nanocomposite (b)

by a larger inhibition zone than the disks with Pal-Ag⁺ for both *E. coli* and *S. aureus* strains. Meanwhile, the MIC of Ag-Pal was lower than that of Pal-Ag⁺ after 24-h incubation (Additional file 4: Table S1). Thus, compared with Pal-Ag⁺ at the same Ag concentration, Ag-Pal exhibited a superior antimicrobial activity. Although Pal-Ag⁺ could slowly release Ag⁺ ions as the antimicrobial agent, the diffusion of Ag⁺ ions might have been hindered by the formation of secondary compounds, such as AgCl in the cultivation medium. In the case of Ag-Pal, the slowly released Ag NPs could freely diffuse into the cultivation medium and act as biocidal agents [24]. Therefore, the synthesized Ag-Pal nanocomposite showed a greater antibacterial activity than Pal-Ag⁺.

Leaching Tests

As one of the most important applications of the studied nanocomposite is the treatment of drinking water, the stability of Ag-Pal in water was evaluated. In the leaching test, vigorous agitation is adopted to ensure that the material is stable under any circumstances occurring in the industrial process. Table 1 shows that the concentration of

Ag in the supernatant was <0.015 mg/L after 12 h, which could be attributed to the stable attachment of the Ag NPs to the Pal matrix. Meanwhile, the obtained results indicate that the nanocomposite is harmless in the case of drinking water treatment, as the amount of leached Ag was significantly lower than the maximum allowable concentration (0.1 mg/L, approved by the World Health Organization) [40]. So, in the water treating process, the Pal-Ag nanocomposite could be used as the excellent contact fungicide when dispersed in the water. Then, clean drinking water could be obtained when the nanocomposite was separated out.

Conclusions

In summary, Ag-Pal nanocomposite was assembled by a rapid and facile UV radiation method ($\lambda = 254$ nm), using CDs derived from wool fiber as a reducing agent. The PXRD spectra and TEM observations confirmed the formation of Ag NPs on the clay surfaces. The antibacterial activity tests revealed that the nanocomposite has a good biocidal effect on both Gram-positive (*S. aureus*) and Gram-negative (*E. coli*) strains, while the leaching

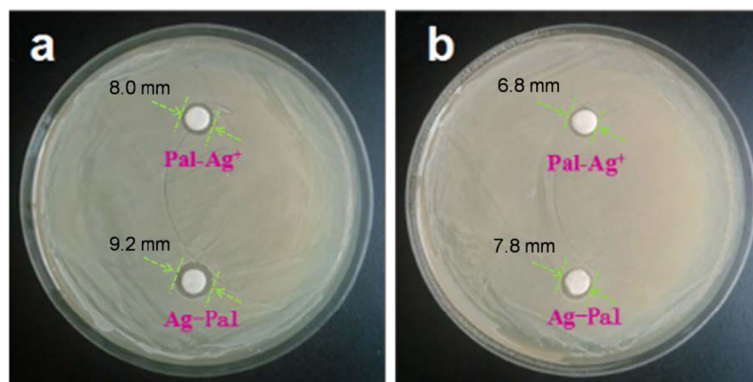


Fig. 6 Representative images of agar plates containing Pal-Ag⁺ and Ag-Pal impregnated disks and diameter of inhibition zone for **a** *S. aureus* and **b** *E. coli*

Table 1 Leaching test results of the Ag-Pal nanocomposite

Sample		0 min	30 min	60 min	4 h	12 h
Ag-Pal	Ag	<0.005	<0.005	<0.005	<0.005	0.015

tests showed that the nanocomposite remained stable under vigorous agitation. Thus, the obtained Ag-Pal nanocomposite is considered to be a promising bactericide with great potential applications.

Additional Files

Additional file 1: Figure S1. EDX spectrum of Pal-Ag⁺. (DOCX 457 kb)

Additional file 2: Figure S2. Flow chart of Ag-Pal synthesis as a function of UV irradiation time. (DOCX 229 kb)

Additional file 3: Figure S3. UV-vis absorption spectra of Ag-Pal nanocomposite in ethanol solution. (DOCX 46 kb)

Additional file 4: Table S1. Minimum inhibitory concentration of Pal-Ag⁺ and Ag-Pal nanocomposite for two microorganisms. (DOCX 16 kb)

Acknowledgements

This work was supported by the National Natural Science Foundation of China (No. 41330317), the Science Foundation of Hebei (No. D2014402046), and the Program for One Hundred Innovative Talents in Universities of the Hebei Province (No. BR2-204). The authors are indebted to Jianjun Liu (Hebei University of Engineering, Handan) for the supplement of lyophilizer.

Authors' Contributions

SH and SQ fabricated all the nanostructures and drafted the manuscript. HZ performed the antibacterial property tests on the composite nanostructures. LK and XL planned the whole work and revised the manuscript. CZ and YJD performed the PXRD tests of the composite nanostructures. All authors read and approved the final manuscript.

Authors' Information

SH worked as a docent in the College of Science, Hebei University of Engineering. His research interests are nanochemistry, nanotechnology, and coordination chemistry. HZ is a Ph.D student in the College of Life Science, Lanzhou University. Her research interests are nanochemistry and biochemistry. Both LK and XL worked as docents in the College of Science, Hebei University of Engineering, their research interests are nanochemistry and nanotechnology. CZ and YD worked as technicians in the College of Science, Hebei University of Engineering, their research interest is nanotechnology. SJQ works as the Dean of the College of Science, Hebei University of Engineering. His research interests are nanobiotechnology and mineral chemistry.

Competing Interests

The authors declare that they have no competing interests.

Author details

¹College of Science, Hebei University of Engineering, Handan 056038, Hebei, People's Republic of China. ²College of Life Science, Lanzhou University, Lanzhou 730000, People's Republic of China. ³Hebei Collaborative Innovation Center of Coal Exploitation, Hebei University of Engineering, Handan 056038, People's Republic of China.

Received: 4 July 2016 Accepted: 20 September 2016

Published online: 27 September 2016

References

- Bhowmick A, Saha A, Pramanik N, Banerjee S, Das M, Kundu PP (2015) Novel magnetic antimicrobial nanocomposites for bone tissue engineering applications. *RSC Adv* 5:25437–45
- Das SK, Khan MMR, Parandhama Laffir F, Guha AK, Sekaran G, Mandal AB (2013) Nano-silica fabricated with silver nanoparticles: antifouling adsorbent for efficient dye removal, effective water disinfection and biofouling control. *Nanoscale* 5:5549–60
- Siddiqi KS, Husen A (2016) Fabrication of metal nanoparticles from fungi and metal salts: scope and application. *Nanoscale Res Lett* 11:98–103
- Talebian N, Zare E (2014) Structure and antibacterial property of nano-SiO₂ supported oxide ceramic. *Ceram Int* 1:281–7
- Wang Y, Xue X, Yang H (2014) Preparation and characterization of carbon or/and boron-doped titania nano-materials with antibacterial activity. *Ceram Int* 8:12533–7
- Wang Y, Xue X, Yang H, Luan C (2014) Preparation and characterization of Zn/Ce/SO₄²⁻-doped titania nano-materials with antibacterial activity. *Appl Surf Sci* 292:608–14
- Maryan AS, Montazer M, Harifi T (2015) Synthesis of nano silver on cellulosic denim fabric producing yellow colored garment with antibacterial properties. *Carbohydr Polym* 22:568–74
- Calderon SV, Ferreri I, Galindo RE, Henriques M, Cavaleiro A, Carvalho S (2015) Electrochemical vs antibacterial characterization of ZrCN-Ag coatings. *Surf Coat Technol* 15:357–62
- Rivero PJ, Urruti A, Goicoechea J, Arregui FJ (2015) Nanomaterials for functional textiles and fibers. *Nanoscale Res Lett* 10:501–23
- Li Y, Chan YC (2015) Effect of silver (Ag) nanoparticle size on the microstructure and mechanical properties of Sn58Bi-Ag composite solders. *J Alloys Compd* 5:566–76
- Eremenko AM, Petrik IS, Smirnova NP, Rudenko AV, Marikvas YS (2016) Antibacterial and antimycotic activity of cotton fabrics, impregnated with silver and binary silver/copper nanoparticles. *Nanoscale Res Lett* 11:28–37
- Motshekga SC, Ray SS, Onyango MS, Momba MNB (2013) Microwave-assisted synthesis, characterization and antibacterial activity of Ag/ZnO nanoparticles supported bentonite clay. *J Hazard Mater* 15:439–46
- Husen A, Siddiqi KS (2014) Phytosynthesis of nanoparticles: concept, controversy and application. *Nanoscale Res Lett* 9:229–53
- Chen X, Dai Y, Wang X (2015) Methods and mechanism for improvement of photocatalytic activity and stability of Ag₃PO₄: a review. *J Alloys Compd* 649:910–32
- Araújo Melo DM, Ruiz JAC, Melo MAF, Sobrinho EV, Martinelli AE (2002) Preparation and characterization of lanthanum palygorskite clays as acid catalysts. *J Alloys Compd* 344:352–5
- Guo H, Zhang H, Peng F, Yang H, Xiong L, Huang C, Wang C, Chen X, Ma L (2015) Mixed alcohols synthesis from syngas over activated palygorskite supported Cu–Fe–Co based catalysts. *Appl Clay Sci* 111:83–9
- Zhang Y, Wang W, Zhang J, Liu P, Wang A (2015) A comparative study about adsorption of natural palygorskite for methylene blue. *Chem Eng J* 15:390–8
- Ogorodova L, Vigasina M, Melchakova L, Krupskaya V, Kiseleva I (2015) Thermochemical study of natural magnesium aluminum phyllosilicate: palygorskite. *J Chem Thermodyn* 89:205–11
- Rajua A, Lakshmia V, Vishnu Prataapb RK, Resmia VG, Rajana TPD, Pavithrana C, Prasada VS, Mohanb S (2016) Adduct modified nano-clay mineral dispersed polystyrene nanocomposites as advanced corrosion resistance coatings for aluminum alloys. *Appl Clay Sci* 126:81–8
- Thongnopkun P, Jamkratoke M, Ekgasit S (2012) Thermal behavior of nano-silver clay in the application of handmade jewelry. *Mater Sci Eng A* 30:849–54
- Saud PS, Pant B, Alam AM, Ghouri ZK, Park M, Kim HY (2015) Carbon quantum dots anchored TiO₂ nanofibers: effective photocatalyst for waste water treatment. *Ceram Int* 41:11953–9
- Barati A, Shamsipur M, Abdollahi H (2015) Hemoglobin detection using carbon dots as a fluorescence probe. *Biosens Bioelectron* 15:470–5
- Muthulingam S, Lee IH, Uthirakumar P (2015) Highly efficient degradation of dyes by carbon quantum dots/N-doped zinc oxide (CQD/N-ZnO) photocatalyst and its compatibility on three different commercial dyes under daylight. *J Colloid Interface Sci* 1:101–9
- Han S, Zhang H, Xie Y, Liu L, Shan C, Li X, Liu W, Tang Y (2015) Application of cow milk-derived carbon dots/Ag NPs composite as the antibacterial agent. *Appl Surf Sci* 328:368–73
- Dao VD, Kim P, Baek S, Larina LL, Yong K, Ryo R, Ko SH, Choi HS (2016) Facile synthesis of carbon dot-Au nanoraspberries and their application as high-performance counter electrodes in quantum dot-sensitized solar cells. *Carbon* 96:139–44
- Ningthoujam RS, Gajbhiye NS (2015) Synthesis, electron transport properties of transition metal nitrides and applications. *Prog Mater Sci* 70:50–154

27. Han S, Liu F, Wu J, Zhang Y, Xie Y, Wu W, Liu W, Wang Q, Tang Y (2014) Targeting of fluorescent palygorskite polyethyleneimine nanocomposite to cancer cells. *Appl Clay Sci* 101:567
28. Ghanwate N, Thakare P, Bhise PR, Gawande S (2016) Colorimetric method for rapid detection of Oxacillin resistance in *Staphylococcus aureus* and its comparison with PCR for *mec A* gene. *Sci Rep* 6:23013–8.
29. Tripathi JK, Pal S, Awasthi B, Kumar A, Tandon A, Mitra K, Chattopadhyay N, Ghosh JK (2015) Variants of self-assembling peptide, KLD-12 that show both rapid fracture healing and antimicrobial properties. *Biomater* 56:92–103
30. Wang Z, Tonderys D, Leggett SE, Williams EK, Kiani MT, Steinberg RS, Qiu Y, Wong IY, Hurt RH (2016) Wrinkled, wavelength-tunable graphene-based surface topographies for directing cell alignment and morphology. *Carbon* 97:14–24
31. Sun DL, Hong RY, Wang F, Liu JY, Rajesh KM (2016) Synthesis and modification of carbon nanomaterials via AC arc and dielectric barrier discharge plasma. *Chem Eng J* 283:9–20
32. Zhang H, Zhao L, Geng F, Guo LH, Wan B, Yang Y (2016) Carbon dots decorated graphitic carbon nitride as an efficient metal-free photocatalyst for phenol degradation. *Appl Catal B Environ* 180:656–62
33. Tu X, Wang L, Cao Y, Ma Y, Shen H, Zhang M, Zhang Z (2016) Efficient cancer ablation by combined photothermal and enhanced chemo-therapy based on carbon nanoparticles/doxorubicin@SiO₂ nanocomposites. *Carbon* 97:35–44
34. Khan MS, Pandey S, Talib A, Bhaisare ML, Wu HF (2015) Controlled delivery of dopamine hydrochloride using surface modified carbon dots for neuro diseases. *Colloids Surf B Biointerfaces* 134:140–6
35. Wang H, Sun P, Cong S, Wu J, Gao L, Wang Y, Dai X, Yi Q, Zou G (2016) Nitrogen-doped carbon dots for “green” quantum dot solar cells. *Nanoscale Res Lett* 11:27–33
36. Li Z, He K, Yin L, Xiong F, Zheng YC (2016) Crystallochemistry of Fe-rich palygorskite from eastern China. *Clay Miner* 42:453–61.
37. Dariani RS, Emami Z (2015) Structural and optical studies of CdS and CdS:Ag nano needles prepared by a SILAR method. *Ceram Int* 41:8820–7.
38. Haneda M, Towata A (2015) Catalytic performance of supported Ag nanoparticles prepared by liquid phase chemical reduction for soot oxidation. *Catal Today* 242:351–6
39. Sarkar B, Liu E, McClure S, Sundaramurthy J, Srinivasan M, Naidu R (2015) Biomass derived palygorskite-carbon nanocomposites: synthesis, characterisation and affinity to dye compounds. *Appl Clay Sci* 114:617–26.
40. Motshekga SC, Ray SS, Onyango MS, Momba MNB (2013) Microwave-assisted synthesis, characterization and antibacterial activity of Ag/ZnO nanoparticles supported bentonite clay. *J Hazard Mater* 262:439–46.

Submit your manuscript to a SpringerOpen[®] journal and benefit from:

- Convenient online submission
- Rigorous peer review
- Immediate publication on acceptance
- Open access: articles freely available online
- High visibility within the field
- Retaining the copyright to your article

Submit your next manuscript at ► springeropen.com
